Rev. Roum. Sci. Techn.– Électrotechn. et Énerg.
Vol. **68**, *2*, pp. 224–231, Bucarest, 2023

MODELING AND SIMULATION OF AN AIRCRAFT ELECTRICAL POWER SYSTEM

OCTAVIAN GRIGORE-MŰLER[1]

Keywords: All-electric aircraft (AEA); Automatic frequency regulator (AFR); Automatic voltage regulator (AVR); Brushless synchronous generator (BSG); Constant speed constant frequency (CSCF); Constant speed drive (CSD); Electrical power systems (EPS); Generator control unit (GCU); Integrated drive generator (IDG); More electric aircraft (MEA); Proportional integral derivative (PID); Synchronous generator (SG); Variable speed constant frequency (VSCF); Variable speed variable frequency (VSVF).

Although recent developments in aircraft electrical technology have had a significant impact on aircraft electrical power systems (EPS), thus reminding the development and production of more electric aircraft (MEA), but also important steps in the development of all-electric aircraft (AEA), still the EPS of the latest aircraft produced by the two big players in the market, the Neo series from Airbus and the NG or Max from Boeing respectively, is completely traditional – a constant speed constant frequency (CSCF) system. Thus, for an alternating current one, it is composed of the power source – the integrated drive generator (IDG), the command and control system – the generator control unit (GCU), the transmission and distribution system, the protection system – the CBs (circuit breaker) and electrical loads. This paper presents the design and simulation of an aircraft EPS using Simulink's Simscape package, a MATLAB program, and for the first time in the specialized literature, a model of the constant speed drive (CSD) generated with the same program is used to drive the synchronous generator (SG) in the IDG.

1. INTRODUCTION

After World War II, many aircraft manufacturing companies were out of business, so they had to turn to the domain of civil transport, mail, and passengers. Thus, the demand for electricity on board the aircraft has continuously increased by increasing aircraft reliability, speed, flight capacity, and comfort.

Since the use of direct current EPS, which was also the first system used on board, was no longer an option due to weight, volume, and power losses on the electrical distribution network, the studies, and research carried out in the early '40s found that an alternating current EPS at a frequency of 400 Hz would be optimal precisely because of the reduced weight for motors and generators without a significant increase in wire weight [1].

As the aerospace electrical industry has pursued the development of power generation systems that best meet the needs of utilization equipment, the salient-pole synchronous generator with wound poles (SG) has been chosen as the standard generator of aircraft EPS precisely because of its advantages inherent in weight, size, performance (the highest electrical output per kilogram per rpm) and efficiency (due to its lowest reactance, transient load performance is the best). How the generator is of the synchronous machine type, the frequency of the AC voltage is proportional to the rotational speed of the generator; some methods of converting the variable engine speed to a constant one are needed when dealing with fixed-frequency systems, so thus the first CSCF electrical power architecture was born. Subsequently, electrical aviation engineers designed and developed other EPS architectures: the variable speed constant frequency (VSCF) technology and, more recently, the variable speed variable frequency (VSVF) technology shown in Fig. 1. In VSCF technology, the electrical power that feeds the loads are generated by some static power converters that are supplied with variable speed/variable frequency power by the direct engine driven generator via a gearbox. Depending on the type of converters, this technology can have three candidates:

- Cycloconverter (cyclo) VSCF that used ac to ac converter;
- Dc link VSCF that used dc to ac converter;
- 270 Vdc VSCF that used ac to dc converter.

In VSVF technology, the electrical power that feeds the loads is generated by a variable frequency generator direct engine driven by the engine via a gearbox. With this technology is equipped MEA, representing about 6.46 % of the commercial airliners in service in 2020 [3, (pp.71)].

But because of the advantages: increased reliability (millions of hours of operation on various aircraft with an MTBF of 30000 hours [2]), lightweight and simple maintenance, the CSCF 115/200 V ac at 400 Hz frequency was chosen to be the standard of the aircraft electrical power system and has remained the same to this day (are equipped about 93.54% from the commercial airliners in service in 2020) [3, (pp.71)].

In a CSCF ac system presented in Fig. 2, the primary power is generated by a three-stage wound-field synchronous generator which is driven at a constant speed by a CSD, which in turn is led by the aircraft engine through a gearbox, at a variable speed, depending on the propulsion power of the engine at different phases of the flight.

From a historical point of view, the probably first major AC EPS was installed on board of the Brabazon Mark I airplane, built by Bristol Aeroplane Company, today BAE Systems Plc. Company, with its first flight on September the 6th, 1949.

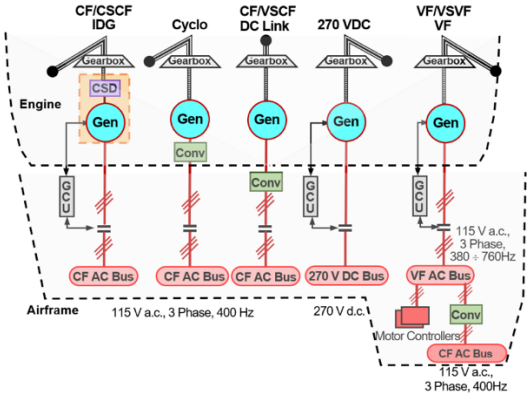

Fig. 1 – The EPS architectures used in aviation.

[1] University POLITEHNICA of Bucharest, Faculty of Aerospace Engineering, Department of Aeronautical Systems Engineering and Aeronautical Management, octavian.grigore@gmail.com

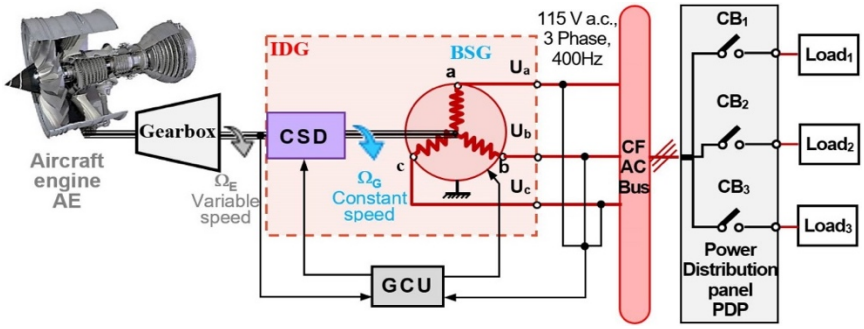

Fig. 2 – The EPS architecture of a CSCF AC system

2. CSD OPERATING PRINCIPLE AND MATHEMATICAL MODEL

The CSD is practically an automatic gearbox that accommodates the variable speed of the aircraft engine to a constant speed needed by the SG. The current CSD based on the Sundstrand patent [4] was developed from Sundstrand Machine Tool Co.'s 1946 direct drive hydraulic CSD installed on board of B-36 bomber by adapting technology from machine tools and oil pumps [2].

The CSD operating principle and its mathematical model have been explained in detail in [5].

3. SYNCHRONOUS GENERATOR MATHEMATICAL MODEL

Starting with the commercial birth of the alternator dated in the last decade of the 19th century, the salient-pole synchronous generator with wound poles had become the standard generator of the electrical industry. That is because it has the highest electrical output per kilogram per rpm of any practical ac generator ever built. Also, its reactances are the lowest of any of the generators, which means that its regulation and performance under transient load conditions are the best of all the ac generators. Due to these advantages, even today, the most present aircraft alternating-current generators are wound-pole, salient-pole synchronous generators.

Thus, it appeared in aviation at the beginning of the 20th century as a source of electrical power for early gyroscope onboard instruments [6, (pp.62)], early communication systems (radiotelephone and radiotelegraph) [7], and early navigation system (blind landing system) [8, (pp.207)], developed in the First World War. At the end of the war, to increase passenger safety, they were introduced into commercial aviation under the name of high-frequency current generator driven most often by a wind turbine [7] and [9], because the engine power was quite low, barely ensuring the lift of the aircraft, and also because its characteristic was not suitable for driving alternators.

From the second decade of the 20th century, with the progress made by the aviation engine manufacturing industry in increasing the specific power of the engine and its reliability, a surplus of power was created that could be used to drive electric generators. However, what led to the introduction of alternators as an energy source for aviation was actually the manufacturing of the first constant speed hydraulic drive in 1946 by Sundstrand Machine Tool Co.

It is well known that the operational reliability and operating lifetime of an electric machine is determined by: the quality of electrical insulation, the quality of bearings and the reliability of the moving contacts (brushes and slip-rings device). As the first two factors depend on the level of technology reached in those fields, the third can be eliminated by using a synchronous generator without moving contacts. The most used solution for this, which has also been used in aviation since 1942, is the synchronous generator with brushless exciter, called brushless synchronous generator (BSG), presented in Fig. 3.

Since long ago the theory of synchronous machines provided several precise mathematical representations of synchronous generators, this paper will be limited to the per unit (*p.u.*) representation only. For determining the equations of a synchronous machine, the following assumptions were taken into account: *i)* the stator windings are sinusoidally distributed along the air gap as long as mutual effects with the rotor are neglected, *ii)* stator slots do not cause appreciable variations in rotor inductances with rotor

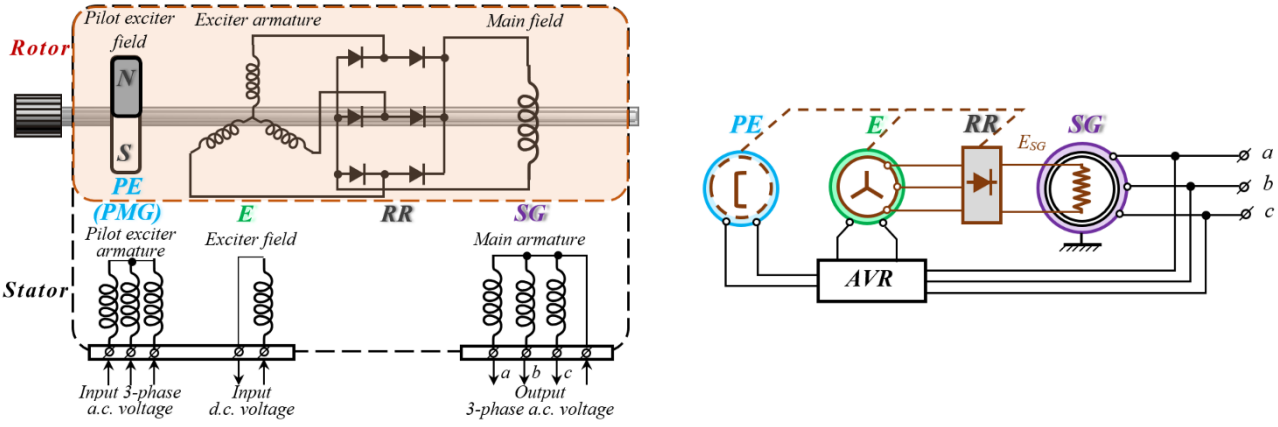

Fig. 3 – The components and schematic diagram of a modern brushless AC generator; *PE* – pilot exciter, a 3-ph SG with permanent magnet (*PMG*); *E* – exciter, a 3-ph SG of inverted construction; *RR* – rotary rectifier; *AVR* – automatic voltage regulator (in *GCU*).

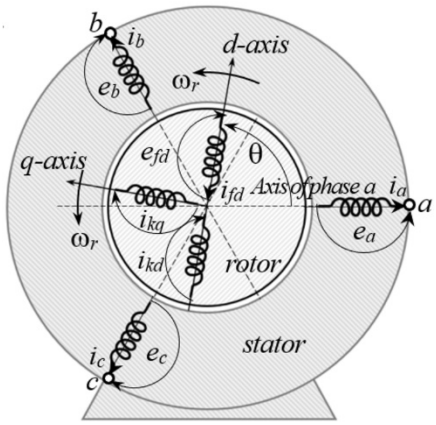

Fig. 4 – SG phase-variable circuit model; *a*, *b*, *c* – stator phase windings; *fd* – field winding; *kd* – d-axis dumper circuit; *kq* – q-axis dumper circuit; *k*=1,*n*, *n* – number pf dumper circuits; θ - angle by which d-axis leads the magnetic axis of phase *a* winding; ω_r – rotor angular speed.

position, *iii)* magnetic hysteresis is negligible, *iv)* magnetic saturation effects are negligible, and v) the currents in the damper, flow in two sets of closed circuits: one whose flow is in line with that of the field along the *d*- axis and the other whose flow is at right angles to the field axis or along the *q*-axis, as is shown in Fig. 4. As the equations of a synchronous machine contain inductance terms which vary with angle θ (angle by which *d*-axis leads the magnetic axis of phase *a* winding in the direction of rotor rotation), which in turn varies with time:

$$\left.\begin{array}{l}\theta = \omega_r t \\ \omega_r = \mathrm{p}\Omega_r \\ \Omega_r = \Omega_{\mathrm{SG}} = \Omega_{\mathrm{CSD}}\end{array}\right\} \Rightarrow \theta = \mathrm{p}\Omega_{\mathrm{CSD}} t, \tag{1}$$

where ω_r is the rotor angular speed (in electrical terms), Ω_r is the mechanical angular velocity, practically the speed with the SG is driven by the CSD, and 2p is the number of poles, a much easiest representation could be obtained by transformation of stator variables, also known the *dq0* transformation. Thus, using Park transformation, $P(\theta)$, the stator voltages, e_a, e_b, e_c, currents i_a, i_b, i_c, and flux linkages ψ_a, ψ_b, ψ_c must be transformed to *dq* rotor orthogonal coordinates. Also, for *p.u.* representation, the variables must be normalized according with:

$$\text{quantity}(p.u.) = \frac{\text{quantity}}{\text{base value of quantity}}. \tag{2}$$

In this case the summary of SG equations in *p.u.* are [10, (pp.84)]:

p.u. stator voltage equations:

$$\begin{aligned} e_d &= \frac{1}{\omega_{base}}\frac{\mathrm{d}\psi_d}{\mathrm{d}t} - \psi_q\omega_r - \mathrm{R_a}i_d \\ \mathrm{e}_q &= \frac{1}{\omega_{base}}\frac{\mathrm{d}\psi_q}{\mathrm{d}t} + \psi_d\omega_r - \mathrm{R_a}i_q\,, \\ e_0 &= \frac{1}{\omega_{base}}\frac{\mathrm{d}\psi_0}{\mathrm{d}t} - \mathrm{R_a}i_0 \end{aligned} \tag{3}$$

where R_a is stator resistance.

p.u. rotor voltage equations:

$$\begin{aligned} e_{fd} &= \frac{1}{\omega_{base}}\frac{\mathrm{d}\psi_{fd}}{\mathrm{d}t} - \mathrm{R_{fd}}i_{fd} \\ 0 &= \frac{1}{\omega_{base}}\frac{\mathrm{d}\psi_{1d}}{\mathrm{d}t} - \mathrm{R_{1d}}i_{1d}\,, \\ 0 &= \frac{1}{\omega_{base}}\frac{\mathrm{d}\psi_{1q}}{\mathrm{d}t} - \mathrm{R_{1q}}i_{1q} \end{aligned} \tag{4}$$

where R_{fd}, R_{1d} and R_{1q} are the resistances of rotor field circuit, *d*-axis damper and *q*-axis damper for winding 1.

p.u. stator flux linkage equations:

$$\begin{aligned} \psi_d &= -(L_{ad}+L_l)i_d + L_{ad}i_{fd} + L_{ad}i_{1d} \\ \psi_q &= -\left(L_{aq}+L_l\right)i_q + L_{aq}i_{1q} \\ \psi_0 &= -L_0 i_0 \end{aligned}\,, \tag{5}$$

where L_l is the stator leakage inductance, L_{ad} and L_{aq} are the mutual inductances of stator *d*-axis and *q*-axis.

p.u. rotor flux linkage equations:

$$\begin{aligned} \psi_{fd} &= L_{ffd}i_{fd} + L_{f1d}i_{1d} - L_{ad}i_d \\ \psi_{1d} &= L_{f1d}i_{fd} + L_{11d}i_{1d} - L_{ad}\,, \\ \psi_{1q} &= L_{11q}i_{1q} - L_{aq}i_q \end{aligned} \tag{6}$$

where L_{ffd} is the self-inductance of the rotor field circuit, L_{11d} and L_{11q} are the self-inductance of the *d*-axis damper, and respectively *q*-axis damper for winding 1; L_{f1d} is the rotor field circuit and *d*-axis damper winding 1 mutual inductance.

*p.u. air-gap torque eq*uation:

$$T = \psi_{\mathrm{d}} i_q - \psi_{\mathrm{q}} i_d. \tag{7}$$

4. CONTROL OF THE SYNCHRONOUS GENERATOR

The operation of aircraft EPS in optimal quality parameters are strictly regulated by several standards [11, 12].

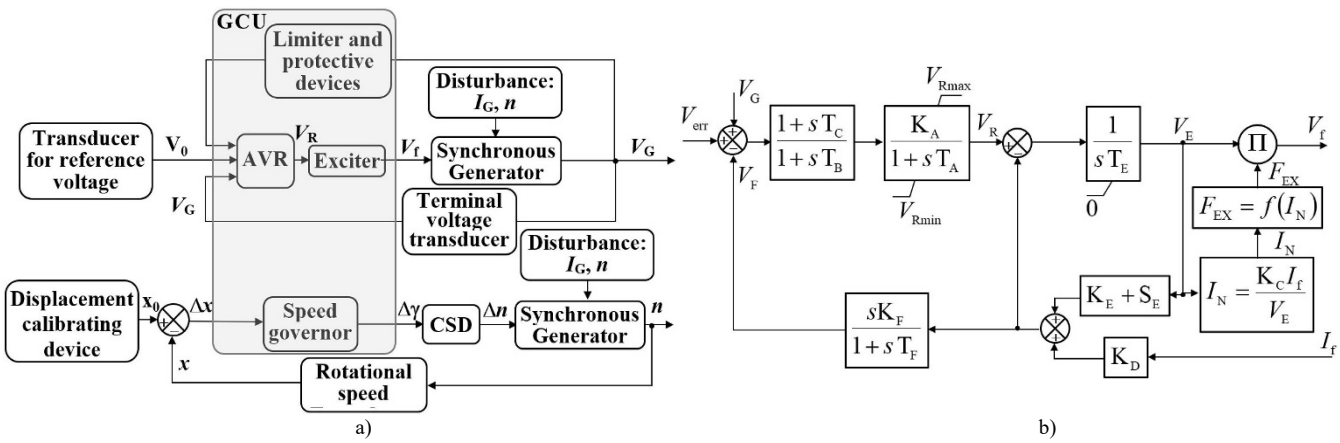

Fig. 5 – a) The control of a BSG; b) Type AC1–A Alternator rectifier excitation system with noncontrolled rectifiers and feedback from exciter field current.

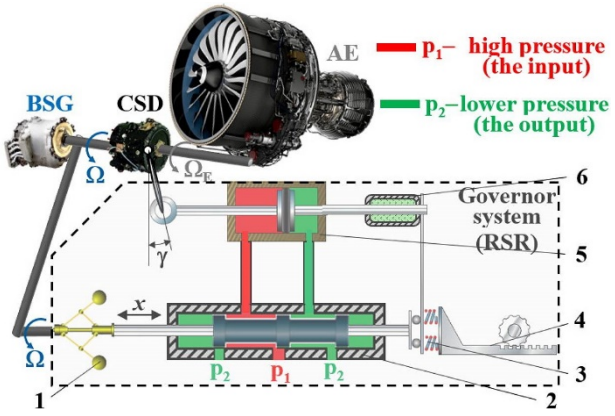

Fig. 6 – Diagram of the RSR or governor system: 1 – centrifugal transducer; 2 – measuring device, the distributor – two-way spool valve; 3 – calibrating device, spring; 4 – the device for tuning the centrifugal element; 5 – hydraulic servomotor; 6 – feedback mechanism.

For an alternating current EPS, among these qualitative parameters, the most important are voltage and frequency.

Since in such a system, the electrical power is generated by a BSG, whose frequency depends on the rotational speed, n, with which the CSD drives it, but also on the load, I_G, the system's frequency must first be controlled.

4.1. AUTOMATIC FREQUENCY REGULATOR (AFR)

The frequency regulation is done through the rotational speed using the CSD or electronic frequency converters. Given that currently, 93.5 4% of existing commercial aircraft in airline fleets use CSD, this paragraph will present the rotational speed regulation with the aid of a rotational speed regulator (RSR) or governor system, shown in Fig. 6. As this device was developed in 1946, its control is of the hydro-mechanical type and due to its advantages explained in the first chapter, the control has remained the same. If the rotational speed of the generator is that imposed by force developed by the centrifugal transducer, 1, along the distributor – 2 this is balanced by the elastic force of the spring 3, the distributor remaining in the middle position blocking the access of the pressurized liquid in the servomotor 5. In the case the rotational speed is different from the rated one, the centrifugal transducer 1 will move distributor 2 to the left or to the right as the rotational speed decreases or increases, thus allowing the circulation of the pressurized liquid to the left or the right of the actuator piston 5, changing the angle of the CSD control device with $\gamma \pm \Delta\gamma$.

For the qualitative study of the process of regulation of RSR, will be studied its components: the centrifugal transducer, the hydraulic servomotor, and the controlled object (CSD and BSG, *i.e.*, IDG).

For the first component at a certain position of the tuning device corresponding to the rated rotational speed of the BSG and at a fixed position of the distributor shaft the equilibrium equation of the forces acting on the distributor shaft can be written:

$$m\frac{d^2x}{dt^2}=\sum_{i=1}^{4}F_i\ , \tag{8}$$

where: m is the mass of the moving parts relative to the distributor shaft and F_i the four forces that act on the shaft: the centrifugal force F_c, the elastic force of the spring F_s, the dry friction force F_f and the viscous force F_{f_v}. In order to obtain the transfer function of the centrifugal transducer the equation (8) must be linearized in a steady state condition, divided by a stabilized reference quantity, passed into operational form and neglected dry friction force and time constant of the centrifugal transducer, it is obtained [3, (pp.259)]:

$$F_1(s)=\frac{x(s)}{\nu(s)}=\frac{K_1}{T_1\cdot s+1}\ , \tag{9}$$

where x is relative displacement of the distributor shaft, respectively, ν the relative variation of the angular velocity of the regulator shaft.

For the second component – the hydraulic servomotor, as the input and output quantities are one-dimensional, it can be considered that the hydraulic actuator is a hydraulic amplifier. So, considering that the volume flow of the liquid circulating in the channels of the regulation system is proportional to the access sectional areas and to the second-order radical of the pressure drops between the outlet and the inlet channels, then it can be written:

$$S_p\frac{dx_p}{dt}=aS_d\sqrt{p_0}\ , \tag{10}$$

where: x_p is the output displacement of the actuator piston, S_p is the area of the servomotor piston, S_d is the area of the distributor passage hole, p_0 the pressure drops of the hydraulic fluid in the channels and a is a proportionality coefficient. Assuming that the operation of the distributor does not have areas of insensitivity, it can be admitted that the speed of movement of the piston is proportional to the displacement, x, i.e.:

$$\frac{dx_p}{dt}=f(x)=k_px\ , \tag{11}$$

with the passage section of the distributor S_d proportional to its displacement, x:

$$S_d=k_dx\ . \tag{12}$$

Then the relation (10) becomes:

$$S_p\frac{dx_p}{dt}=ak_dx\sqrt{p_0}\ . \tag{13}$$

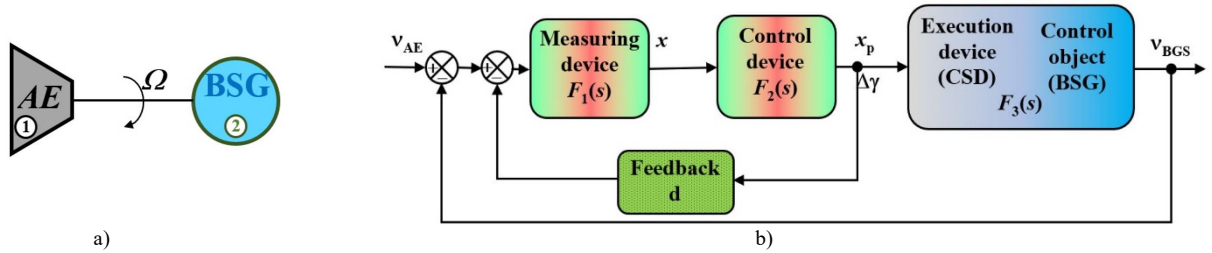

Fig. 7 – a) The driven generator model; b) the RSR diagram.

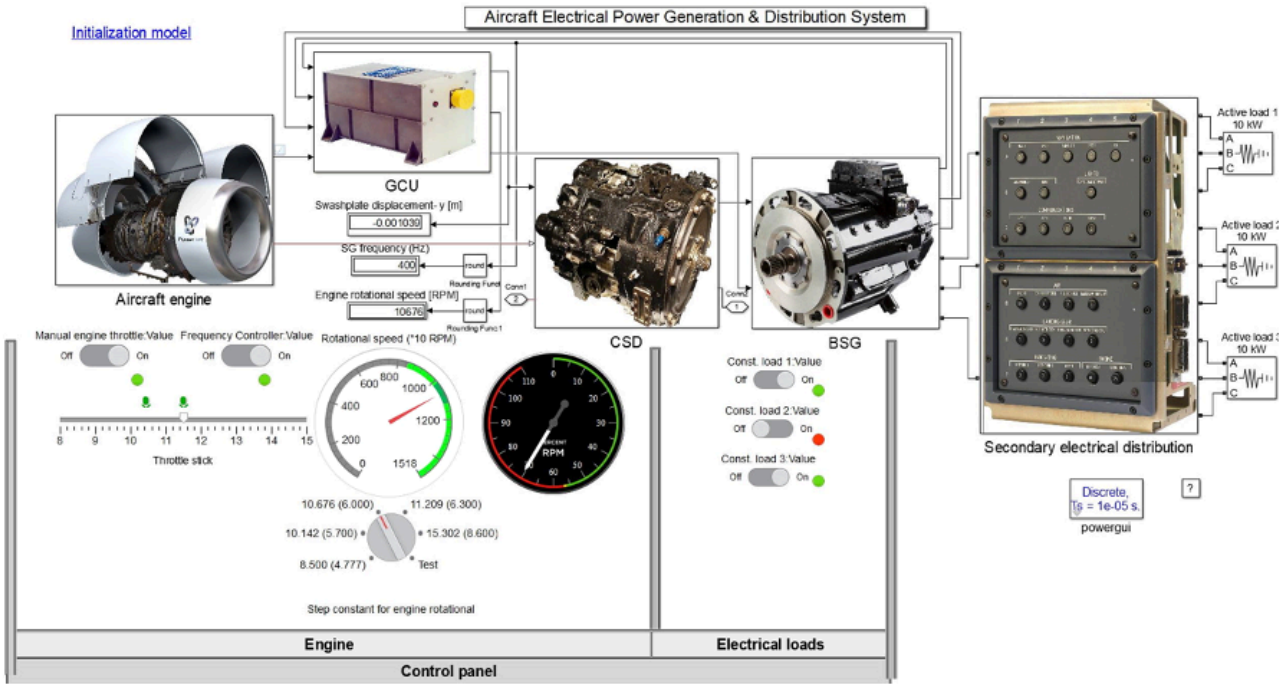

Fig. 8 – Aircraft electrical power generation and distribution system Simulink model.

Applying the same operation like for the first component, applying small deviations of the variables, divided by a stabilized reference quantity and transformed it into operational form, was obtained:

$$S_p X_{p_0} s \frac{\Delta X_p(s)}{X_{P_0}} = a\sqrt{p_0} k_d X_0 \frac{\Delta X(s)}{X_0} \Leftrightarrow$$
$$\Leftrightarrow T_2 s x_p(s) = K_2 x(s) , \quad (14)$$

where: $T_2 = S_p X_{p_0}$ is the time constant of servomotor;

$K_2 = a\sqrt{p_0} k_d X_0$ a constant of proportionality;

$x_p(s) = \frac{\Delta X_p(s)}{X_{P_0}}$ the relative variation of the actuator piston displacement.

In this case the transfer function of the hydraulic actuator given by eq. (14) becomes:

$$F_2(s) = \frac{x_p(s)}{x(s)} = \frac{K_2}{s \cdot T_2} , \quad (15)$$

that is, an integrating element.

To determine the equation of the third component it was consider the steady state operation of a generator driven by the aircraft engine like is represented in Fig. 7 a). Applying the Newton's second law related to the drive shaft is obtained:

$$M_1 = M_2 + M_{Dynamic} = M_2 + J \frac{d\Omega}{dt} . \quad (16)$$

As the motor torque of the AE, M_1, depends on the rotation velocity, Ω, command, z, and disturbance, Q:

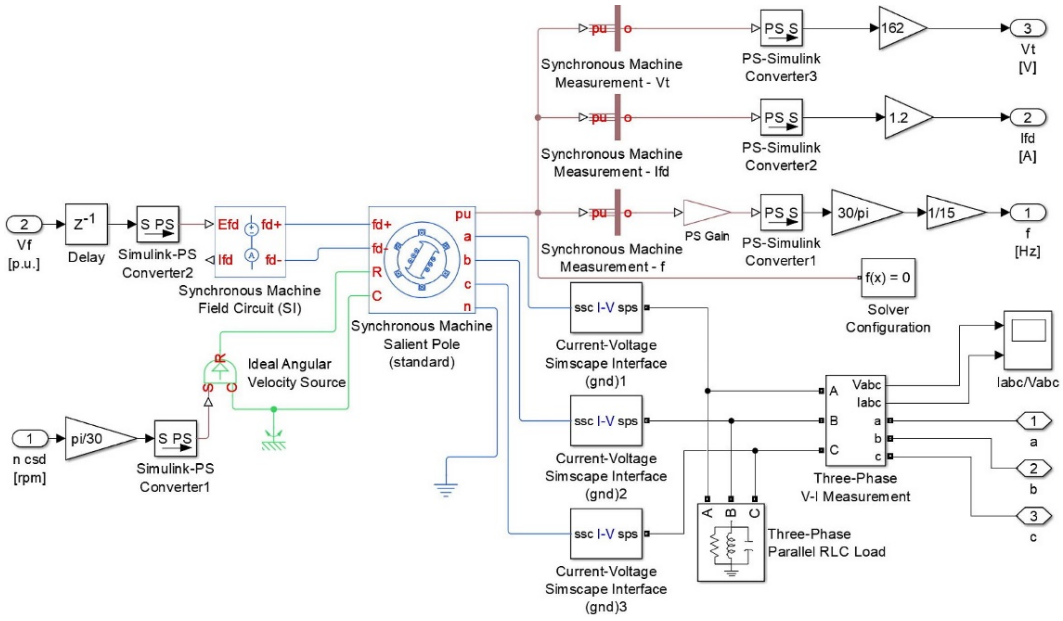

Fig. 9 – BSG Simulink model.

$$M_1=M_1(\Omega,z,Q)\,, \tag{17}$$

the torque of the BSG, M_2, depends on electromagnetic power, P, and mechanical angular velocity, Ω:

$$M_2=M_2(\Omega,P)\,, \tag{18}$$

passing relation (16) into the dimensionless variables by dividing it with the stabilized torque M_0, and transforming it into operational form yields [3, (pp.178)]:

$$\mathrm{T}s\nu(s)+\mathrm{S}\cdot\nu(s)=\mathrm{N}\cdot\sigma(s)+\lambda\cdot q(s)-p_e(s). \tag{19}$$

Because the variation of the electromagnetic power is small $p_e(s)\cong 0$ and due to the CSD, the variations of the disturbances on the drive aircraft engine are approximately zero $q\cong 0$, then (19) becomes:

$$(\mathrm{T}s+\mathrm{S})\nu(s)=\mathrm{N}\cdot\sigma(s), \tag{20}$$

with the transfer function:

$$F_3(s)=\frac{\nu(s)}{x_p(s)}=\frac{\mathrm{N}}{\mathrm{T}\cdot s+\mathrm{S}}=\frac{\mathrm{N}`}{\mathrm{T}`\cdot s+1}\,. \tag{21}$$

Finally, using the control diagram from Fig 7 b), the transfer function of regulating system is:

$$F(s)=\frac{\mathrm{K}}{\mathrm{T}_1\mathrm{T}`_2\mathrm{T}`_M s^3+(\mathrm{T}_1\mathrm{T}`_2+\mathrm{T}`_2\mathrm{T}`_M)s^2+(\mathrm{T}`_2+\mathrm{T}`_M)s+1+\mathrm{K}}\,, \tag{22}$$

with $\mathrm{K}=\mathrm{K}`_{12}\mathrm{N}`$, $\mathrm{K}`_{12}=1/\mathrm{d}$ and $\mathrm{T}`_2=\mathrm{T}_2/(\mathrm{d}\mathrm{K}_1\mathrm{K}_2)$.

4.2. AUTOMATIC VOLTAGE REGULATOR (AVR)

The accurate operation of a synchronous machine depends largely on the exact design of its excitation system and the voltage transducer and voltage regulator. To assist manufacturers of electric machines and their components, the IEEE Society developed the standard IEEE Std 421.5 [13], in which models for the excitation system of synchronous generators and models for their control were included. According to it, a synchronous machine's general functional block diagram, shown in Fig. 5, includes the following subsystems: a terminal voltage transducer, an exciter system, an automatic voltage regulator, and a protection device. Models for all of these are presented in the recommended practice of the standard. Thus, three distinct types of excitation are identified for the exciter:

- Type DC, which uses a dc generator as the source of direct current for the BSG field;
- Type AC uses an ac generator and a stationary or rotating rectifier to obtain the direct current;
- Type ST (static) in which excitation current is supplied using transformers or auxiliary generator windings and rectifiers.

Since all the generators installed in the airliners in service are based on the generator developed by the Westinghouse company [14], among all three excitation modes according to [13], the Type AC1A was chosen. The model of this exciting type is shown in Fig. 5 b), where the parameters are: F_{EX} rectifier loading factor, a function of I_N, I_f synchronous machine field current, I_N normalized exciter load current, V_E exciter voltage back commutating reactance, V_{err} voltage error signal, V_f exciter output voltage, V_F excitation system stabilizer output, V_G terminal voltage, V_R voltage regulator output, T_A, T_B and T_C voltage regulator time constants, T_E exciter time constant, T_F damping filter time constant, K_A voltage regulator gain, K_C rectifier loading factor, K_D demagnetizing factor, K_E exciter constant, K_F damping filter gain and S_E exciter saturation function.

3. SIMULATION AND RESULTS

The B737-300, the subject of this paper's simulation, is part of the classic generation. Since its launch in 1984, 1113 units have been produced [15], of which 109 are still flying in the world's fleets today [16].

To validate the Simulink model of the EPS, the B737-300 electrical power generation and distribution system shown in Fig. 8 were developed. The system is composed of the aircraft engine model, the CSD model, the BSG model, the generator control unit (GCU) model, which has the role of

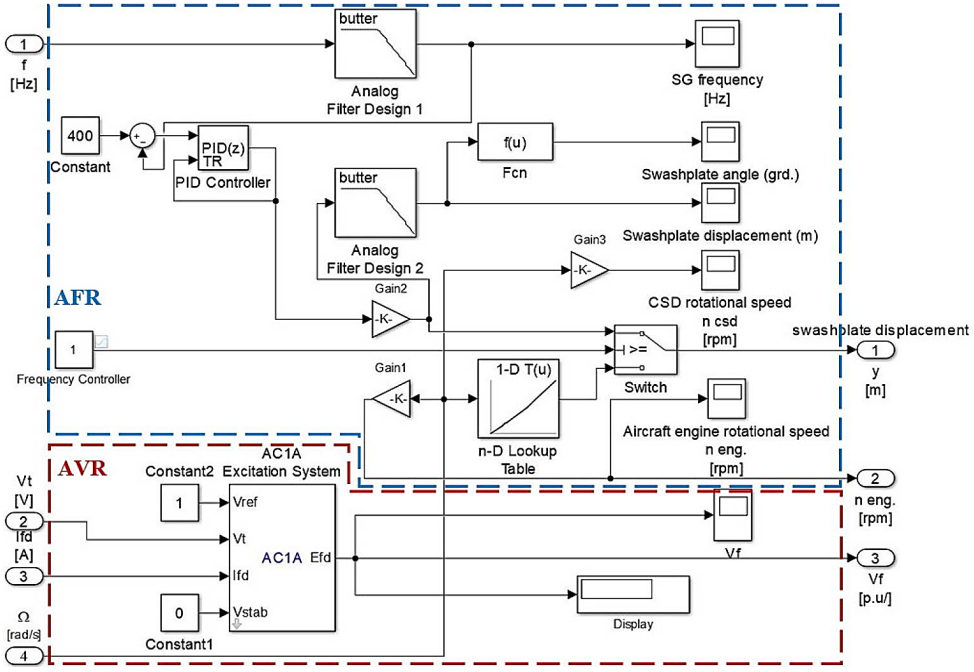

Fig. 10 – GCU Simulink model.

regulating the voltage with the help of BSG excitation and the frequency with CSD, and the last block is the secondary electrical distribution with its loads.

This topic is addressed in the specialized literature using Matlab/Simulink [17, 18], or with the simulation made in other programming languages (Saber [19, 20], ANSYS Simplorer [21, 22,], Amesim [23], SimVimCockpit [24]), but the generator is driven from a constant torque, never using the CSD, as it is in reality, and with the help of which the automatic control of the rotational speed, respectively of the frequency is also done.

The model of the electrical power generation and distribution system of the B737-300 aircraft is performed in Simulink / Matlab v.9.0. The input data, the parameters of the aircraft engine, were presented in detail in [5], where the Simulink model of the CSD was also explained.

However, for compliance, the input data with which the mechanical aircraft engine profile was generated and presented in Fig. 11 are: the engine rotational speed is between 8000 and 13500 rpm, with acceleration and deceleration of the drive motor between 50 and 800 rpm/s, also, rotational speed must stabilize within 3 to 6 s, with a maximum error of ± 2%.

The Simulink model of the BSG is presented in Fig. 9. It contains the model of a standard synchronous machine with salient poles, the field circuit of the synchronous machine, and auxiliary blocks for transforming, measuring and amplifying signals. It should be noted that the generator model presented in section 3 is actually made up of the two models mentioned above, but also of the excitation model AC1A Excitation System from GCU.

The main parameters of B737-300 3-phase 8 poles SG rated at 40 kVA are represented in Table 1 [25].

The GCU that was represented in Fig. 10 contains the AFR and AVR. The frequency must be regulated first for the proper operation of the BSG. Although the rotational speed regulation of the BSG is made mechanically by the CSD, as was presented in Section 4.1, there is also a fine-tuning of the frequency (called trimming) done electrically using an electromagnet that drives the servomotor shaft. Thus, the AFR was made with a tuned PID controller so that the frequency had the quality parameter from [13]. The AVR was done with the AC1A excitation system.

To fit the qualitative parameters of the BSG voltage in [13], the parameters of the AC1A controller were tuned as follows: the first time, the idle voltage is adjusted with the help of K_A to obtain the maximum allowed value. When running under the maximum admissible load, check that V_f is at the maximum value. Overshoot and settle time adjustment is done with T_F. Figure 11 represents the simulation results, first with the AFR decoupled for the first 9 seconds, and then, when the speed exceeds the nominal value, it is engaged. The overshoot can be explained by the initial conditions being different from the engagement time. In the second scenario, the AFR is engaged from the start, settling in less than one second, and is disengaged at second 17.5 to demonstrate its operation. Even now, the proper operation of the AVR can be seen by connecting the load at 4 and 7.5 seconds and disconnecting it at 10 and 12.5 seconds, with voltage stabilization in less than 0.5 seconds without exceeding the imposed limits. Also, from the figure, we can see the good regulation of the terminal voltage, which remains between the two limits regulated by the standard [11], regardless of the variation in the drive speed of the BSG and the load variations connected to its terminals.

Table 1

GS parameters

Nr. crt.	Quantity	Symbol	*p.u.* value
1.	Direct-axis synchronous reactance	X_d	1.50
2.	Leakage reactance	X_l	0.11
3.	DC resistance	R_a	0.024
4.	Quadrature-axis synchronous reactance	X_q	0.91
5.	Direct-axis transient reactance	X'_d	0.15
6	Direct-axis subtransient reactance	X''_d	0.15
7	Quadrature-axis subtransient reactance	X''_q	0.54
8.	Zero-sequence impedance	Z_0	$0.024+0.043j$

11. **CONCLUSIONS**

This paper presents for the first time in a specialized paper a simulation with the Simulink/Matlab of an aircraft EPS that uses a CSD to drive the BSG, just as it happens otherwise in reality. Using the scenario from [5], it can be seen that frequency and terminal voltages are well regulated, both to the variation of the load and the rotational speed. Some of the challenges were to tune both frequency and voltage regulators to obtain the qualitative parameters of energy as regulated by standards.

Received on (month day, year)

REFERENCES

1. T.B. Holliday, *Applications of Electric Power in Aircraft*, Electrical Engineering, **60**, 5, pp. 218 – 225, May 1941.
2. A.K. Hyder, *A Century of Aerospace Electrical Power Technology*, Journal of Propulsion and Power, **19**, 6, pp. 1155 (2003).
3. O. Grigore-Müler, *Aircraft electrical power system. Analysis and design*, Matrix ROM, București, România (2021).
4. C.J. Gantzer, *Combined fluid and mechanical drive*, US3365981A patent, 30.01 (1968).
5. O. Grigore-Müler, *Modeling of an aircraft constant speed drive*, Revue Roumaine des Sciences Techniques, **67**,4, pp. 487–492 (2022).
6. R.G. Grant, *Flight - 100 years of aviation*, Dorling Lindresley Ltd., A Penguin Company (2002).
7. L.A. Hyland, *Airplane Radio Sets*, Aviation, **XXIII**, 26, pp. 1526, 26 December 1927.
8. *The Aircraft Year Book for 1935*, Aeronautical Chamber of Commerce of America, **17** (1919).
9. E.A. Sperry, *Wind-driven generator for aircraft*, US1362753 patent, 21.12 (1920).
10. P. Kundur, *Power system stability and control*, McGraw-Hill, USA (1994).
11. *Aerospace – Characteristics of aircraft electrical systems,* ISO1540, 3rd Ed., 2006.
12. *Aircraft electric power characteristics,* MIL-STD-704F w/CHANGE 1 (2004).
13. *IEEE Recommended practice for excitation system models for power system stability studies,* IEEE Std 421.5 (2016).
14. H.D. Else, D.R. Basel, H.J. Braun, S. Township, *Liquid-cooled dynamoelectric machine*, US2862119 patent, 25.11 (1958).
15. *Orders & Deliveries, Revenue Recognition Accounting Standard ASC 606 Information,* Orders through 01/31/2023, Boeing Company.
16. J. Hardiman, *Which airlines still fly the Boeing 737-300*, Canadian Aviation News, 25/09/2021.
17. A.A. Efimov, S.Yu. Melinkov, A.G. Garganeev, *Simulation of aircraft electrical power supply system*, 2108 IV International Conference on Information Technologies in Engineering Education, Russia, 23-26 October 2018.
18. A. Tantawy, X. Koutsoukos, G. Biswas, *Aircraft generators: Hybrid Modeling and simulation for fault detection,* IEEE Transaction on Aerospace and Electronic Systems, **48**, 1, pp. 552–571 (2012).
19. F.M. Bruck, F.A. Himmelstoss, *Modelling and simulation of a synchronous machine*, COM.P.EL.98. Record 6th Workshop on Computer in Power Electronics, Italy, 22 July 1998.

20. M. Michna, F. Kutt, P. Chrzan, M. Ronkowski. *Modeling and analysis of a synchronous generator in more electric aircraft power system using synopsys/Saber simulator*, Prace Elektrotechniki, 240, pp/ 31-46 (2009).
21. X. Li, S. Kher, S. Huang, V. Ambalavanar, Y. Hu, *Component modeling and system level simulation of aircraft electrical systems*, Engineering Letters, **24**, 2, pp. 178–186 (2016).
22. T. Kurtoglu, P. Bunus J. De Kleer, R. Rai, *Simulation-based design of aircraft electrical power systems*, Linköping Electronic Conference Proceedings, **63**, pp. 704–712 (2011).
23. G. Dinesh, B. Viswa Adithya, V. Vedula, *Modeling of a traditional aircraft generator and its subsystems*, 2015 IEEE International Conference on Electrical, Computer and Communication Technologies, India, 5-7 March 2015.
24. L. Ruiz, G. Inca, R. Bautista, E. Arevalo, *Simulation of a Boeing 737-500 Aircraft Electrical System*, 2022 IEEE Sixth Ecuador Technical Chapters Meeting, Ecuador, 11-14 October 2022
25. L.J. Stratton, L.W. Matsch, *Characteristics of aircraft a-c generators,* Transactions of the American Institute of Electrical Engineers, Part II: Applications and Industry, **73**, 4, pp. 165–169 (1954).

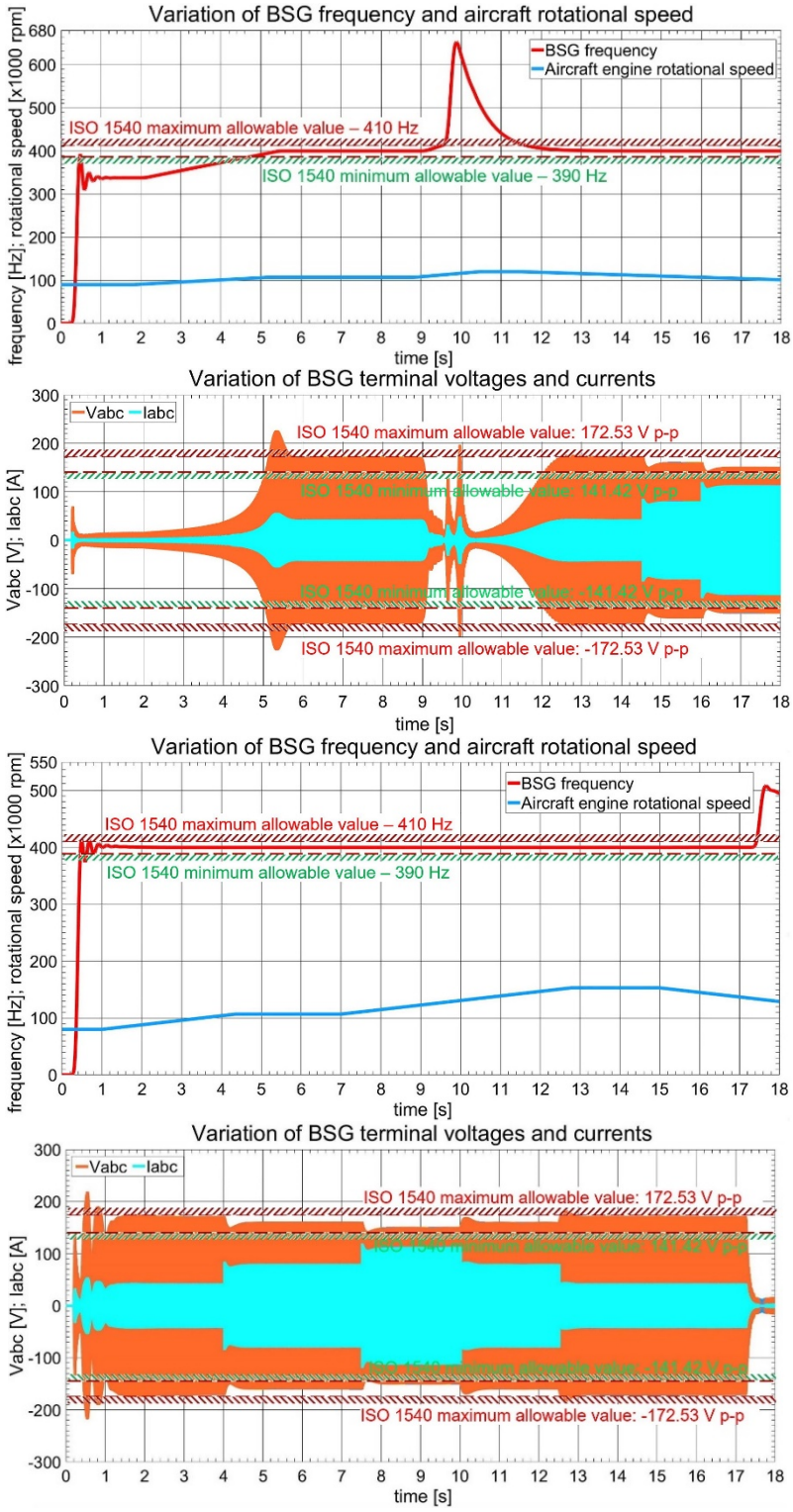

Fig. 11 – Characteristics of the aircraft engine and BSG.